 Related Commentary, page 1450

Aberrantly glycosylated IgA1 in IgA nephropathy patients is recognized by IgG antibodies with restricted heterogeneity

Hitoshi Suzuki,[1,2] Run Fan,[1,3] Zhixin Zhang,[3] Rhubell Brown,[1] Stacy Hall,[1] Bruce A. Julian,[1,4] W. Winn Chatham,[4] Yusuke Suzuki,[2] Robert J. Wyatt,[5] Zina Moldoveanu,[1] Jeannette Y. Lee,[6] James Robinson,[7] Milan Tomana,[4] Yasuhiko Tomino,[2] Jiri Mestecky,[1,4,8] and Jan Novak[1]

[1]Department of Microbiology, University of Alabama at Birmingham, Birmingham, Alabama, USA. [2]Division of Nephrology, Department of Internal Medicine, Juntendo University School of Medicine, Tokyo, Japan. [3]Department of Pathology and Microbiology, University of Nebraska Medical Center, Omaha, Nebraska, USA. [4]Department of Medicine, University of Alabama at Birmingham, Birmingham, Alabama, USA. [5]Department of Pediatrics, University of Tennessee Health Sciences Center, Memphis, Tennessee, USA. [6]Department of Biostatistics, University of Arkansas for Medical Sciences, Little Rock, Arkansas, USA. [7]Department of Pediatrics, Tulane University, New Orleans, Louisiana, USA. [8]Institute of Microbiology and Immunology, First Faculty of Medicine, Charles University, Prague, Czech Republic.

IgA nephropathy (IgAN) is characterized by circulating immune complexes composed of galactose-deficient IgA1 and a glycan-specific IgG antibody. These immune complexes deposit in the glomerular mesangium and induce the mesangioproliferative glomerulonephritis characteristic of IgAN. To define the precise specificities and molecular properties of the IgG antibodies, we generated EBV-immortalized IgG-secreting lymphocytes from patients with IgAN and found that the secreted IgG formed complexes with galactose-deficient IgA1 in a glycan-dependent manner. We cloned and sequenced the heavy- and light-chain antigen-binding domains of IgG specific for galactose-deficient IgA1 and identified an A to S substitution in the complementarity-determining region 3 of the variable region of the gene encoding the IgG heavy chain in IgAN patients. Furthermore, site-directed mutagenesis that reverted the residue to alanine reduced the binding of recombinant IgG to galactose-deficient IgA1. Finally, we developed a dot-blot assay for the glycan-specific IgG antibody that differentiated patients with IgAN from healthy and disease controls with 88% specificity and 95% sensitivity and found that elevated levels of this antibody in the sera of patients with IgAN correlated with proteinuria. Collectively, these findings indicate that glycan-specific antibodies are associated with the development of IgAN and may represent a disease-specific marker and potential therapeutic target.

Introduction

IgA nephropathy (IgAN), also called Berger disease, was described in 1968 (1) based on the immunohistochemical finding of IgA- and IgG-containing immune complexes in the glomerular mesangium of the kidney. Proliferation of mesangial cells and expansion of the extracellular matrix can occur from the earliest stages of the disease, with progression to glomerular and interstitial sclerosis resulting in development of end-stage renal disease in 30%–40% patients within 20 years of the estimated time of disease onset (2, 3).

The IgA in the mesangial deposits is exclusively of the IgA1 subclass (4–6) and is aberrantly glycosylated (7–9) with the hinge-region *O*-linked glycans being deficient in galactose (Gal) (10–14). The IgA1 in the circulation of patients with IgAN also carries Gal-deficient *O*-glycans, although Gal-deficient variants are rarely found in the IgA1 in sera from normal individuals (7–9, 15). The production of these variants is due to altered expression of specific glycosyltransferases in the IgA1-producing cells (16–19).

It is the binding of IgA1-containing immune complexes with aberrantly glycosylated IgA1 (11–13, 20–22) to mesangial cells that induces the renal manifestations characteristic of IgAN (23–26); however, the events that initiate the disease process are most likely of extrarenal origin, as IgAN recurs in more than 50% of patients within 2 years of kidney transplantation (27). Thus, the factors that favor the formation of the circulating immune complexes in these patients are of particular interest. Although it is known that the aberrantly glycosylated IgA1 is recognized by glycan-specific antibodies of the IgG or IgA1 isotypes from patients with IgAN as well as from healthy individuals (13, 21, 28–30), little is known concerning the precise specificities and molecular properties of the antibodies.

EBV-immortalized Ig-producing cells from IgAN patients and healthy controls offer what we believe is a novel tool for characterization of the anti-IgA1 antibodies as well as IgA1 glycosylation (19, 30). In the present study, we subcloned IgG-producing cells from IgAN patients, healthy controls, and non-IgAN renal-disease controls, generated stable single-cell clones producing IgG specific for Gal-deficient IgA1, and characterized these antibodies at the molecular level. Subclones of EBV-immortalized B lymphocytic cell lines from IgAN patients produced IgG that formed complexes with Gal-deficient IgA1. Sequencing of the cloned heavy- and light-chain antigen-binding domains of IgG specific for Gal-deficient

Conflict of interest: The authors have declared that no conflict of interest exists.

Nonstandard abbreviations used: CDR3, complementarity-determining region 3; dd-IgA1, desialylated and degalactosylated IgA1; D_H, diversity region of *IGH* gene; Fab-IgA1, Fab fragment of Gal-deficient IgA1 containing the N-terminal part of the hinge region with *O*-glycans; Gal, galactose; GalNAc, *N*-acetylgalactosamine; HAA, *Helix aspersa* agglutinin; HR-BSA, synthetic IgA1 hinge-region peptide linked to BSA; HR-GalNAc-BSA, synthetic IgA1 hinge-region glycopeptide linked to BSA with 3 GalNAc residues; IgAN, IgA nephropathy; J_H, joint region of *IGH* gene; rIgG, recombinant human IgG; ROC, receiver operating characteristic curve; UP/Cr, urinary protein/urinary creatinine (ratio); V_H, variable region of *IGH* gene.

Citation for this article: *J. Clin. Invest.* **119**:1668–1677 (2009). doi:10.1172/JCI38468.

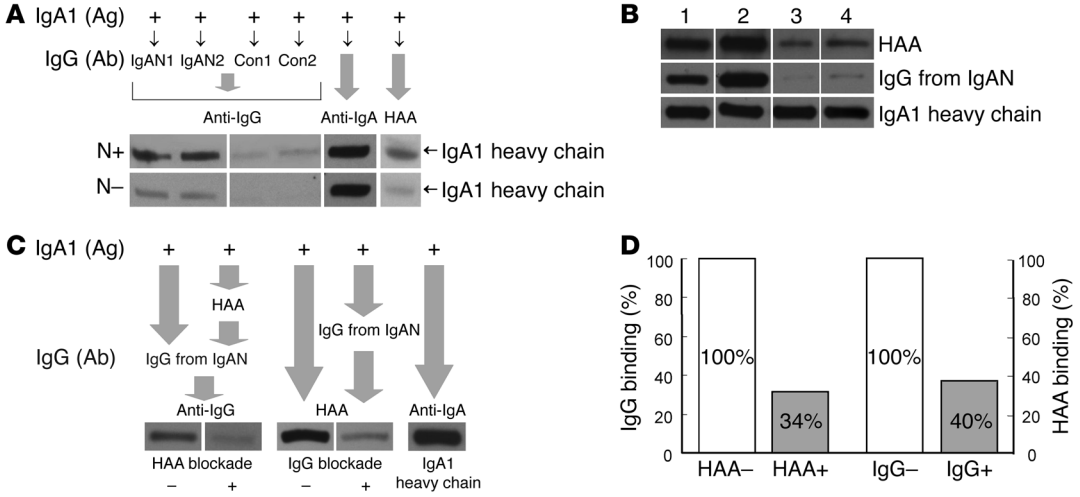

Figure 1

Serum IgG from IgAN patients exhibits specificity for GalNAc, binding to Gal-deficient and desialylated IgA1. (**A**) Western blot analysis with Gal-deficient IgA1 (Mce) as antigen demonstrated binding of serum IgG from 2 IgAN patients but only minimal binding of IgG from 2 healthy controls to the IgA1 heavy chain. After removal of sialic acid, IgG binding increased, as it did for binding to HAA. N+, treated with neuraminidase; N-, not treated with neuraminidase. (**B**) To test glycan-specific IgG binding to GalNAc, these IgA1 proteins were used: lane 1, Gal-deficient IgA1 (Mce); lane 2, dd-IgA1; lane 3, enzymatically regalactosylated dd-IgA1; and lane 4, enzymatically resialylated dd-IgA1. dd-IgA1 bound the greatest amount of HAA, with enzymatically galactosylated or sialylated dd-IgA1 binding very little. IgG from an IgAN patient bound to these antigens in a fashion similar to that for HAA. (**C** and **D**) Component chains of Gal-deficient IgA1 (Mce) were separated by SDS-PAGE under reducing conditions and electroblotted. The membrane was then treated with HAA to assess whether blockade with this GalNAc-specific lectin can inhibit IgG binding. The intensity of each band was quantified by densitometry. The binding of serum IgG from an IgAN patient to Gal-deficient IgA1 was reduced by 66% after treatment with HAA. Conversely, blocking with serum IgG from an IgAN patient reduced the binding of HAA to Gal-deficient IgA1 by 60%. Binding of anti-human IgA (heavy-chain specific) confirmed equivalent loading. Representative results from 3 experiments are shown in **A**–**C**; lanes were run on the same gel but were noncontiguous.

IgA1 identified in IgAN patients an A to S substitution in the complementarity-determining region 3 (CDR3) of the variable region of the IgG heavy chain; site-directed mutagenesis confirmed the role of the serine residue in binding to Gal-deficient IgA1. Thus, the anti-glycan antibodies with unique features in the CDR3 are associated with the development of IgAN.

Results

Serum IgG from IgAN patients exhibits specificity for N-acetylgalactosamine, which results in binding with Gal-deficient and desialylated IgA1. We first determined the binding of serum IgG from IgAN patients to Gal-deficient IgA1 using an ELISA in which the coated antigen was either enzymatically desialylated and degalactosylated IgA1 (dd-IgA1) or the Fab fragment of Gal-deficient IgA1 containing the N-terminal part of the hinge region with *O*-glycans attached (Fab-IgA1) (Supplemental Table 1; supplemental material available online with this article; doi:10.1172/JCI38468DS1). The levels of serum IgG directed against dd-IgA1 and Fab-IgA1 were higher in IgAN patients than in healthy controls ($P < 0.001$) (Supplemental Table 2). These results, obtained using samples from 16 patients and 16 healthy controls from the southeastern USA, were corroborated using serum samples from 20 IgAN patients and 20 healthy controls from Japan ($P < 0.0001$) (Supplemental Table 2).

The binding of the serum IgG to Gal-deficient IgA1 was then validated by Western blot analysis of the component chains of an enzymatically modified IgA1 myeloma protein (Mce). In each case, the enzymatic modification was confirmed by the binding of the *N*-acetylgalactosamine–specific (GalNAc-specific) lectin, *Helix aspersa* agglutinin (HAA) (31, 32). The IgG from the sera of patients with IgAN bound to the heavy chain of the Gal-deficient IgA1, whereas only minimal binding of the IgG from the sera of healthy controls was observed. Removal of the sialic acid from the Gal-deficient IgA1 by neuraminidase treatment resulted in an increase in the binding of the serum IgG from patients with IgAN (Figure 1A). As would be expected, dd-IgA1 bound greater amounts of HAA than did native Gal-deficient IgA1, whereas enzymatically regalactosylated or resialylated dd-IgA1 bound lower amounts of HAA than native Gal-deficient IgA1 (Figure 1B). The similarity between the extent of binding of the serum IgG and HAA to each of these IgA1 preparations suggested that the binding of serum IgG to the Gal-deficient IgA1 was dependent on the GalNAc moieties (Figure 1B). This was confirmed by incubation with unlabeled HAA prior to incubation with IgG purified from the serum of an IgAN patient. The preincubation with HAA reduced the binding of the IgG to the Gal-deficient IgA1 by 66% (Figure 1, C and D); conversely, blocking with serum IgG from an IgAN patient reduced the binding of HAA to Gal-deficient IgA1 by 60% (Figure 1, C and D). Thus, the GalNAc in the hinge region of Gal-deficient IgA1 represents a major component of the epitope that is recognized by the IgG specific for Gal-deficient IgA1 present in the serum of patients with IgAN.

Characterization of antibodies specific for Gal-deficient IgA1 secreted by IgG-producing cell lines. To further characterize the IgG that reacts with the Gal-deficient IgA1, we generated IgG-producing cells by EBV immortalization of B cells isolated from the peripheral blood of the 16 patients with IgAN and 16 healthy controls who had provided blood for measurement of serum IgG specific for Gal-deficient IgA1 (Supplemental Table 2). After subcloning of the cells, the IgG secreted by the cell lines was characterized by ELISA; the cells

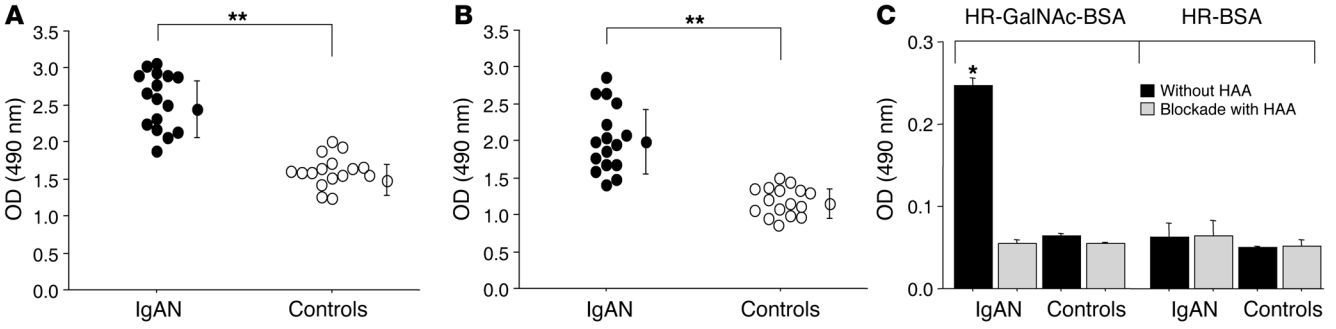

Figure 2

Characterization of antibodies specific for Gal-deficient IgA1 secreted by cloned cell lines. The levels of antigen-specific IgG produced by IgG-secreting cell lines were measured by capture ELISA. The results are expressed as OD measured at 490 nm. Levels of IgG directed against dd-IgA1 (**A**) and Fab-IgA1 (**B**) were higher in IgAN patients than in controls. Each group, $n = 16$. $^{**}P < 0.0001$; data are shown as individual values and mean ± SD. (**C**) IgG secreted by cell lines from IgAN patients and healthy controls (each group, $n = 10$) was tested for binding with a hinge-region glycopeptide (HR-GalNAc-BSA) or HR-BSA, with or without HAA blockade. IgG produced by cell lines from IgAN patients bound to HR-GalNAc in an HAA-inhibitable fashion. $^{*}P < 0.001$; data are shown as the mean ± SD. *P* values were generated using 2-tailed Student's *t* test. The experiments were repeated 3 times with similar results.

derived from IgAN patients produced antibodies that exhibited greater binding to dd-IgA1 and Fab-IgA1 than did the cells derived from controls ($P < 0.0001$) (Figure 2, A and B). We then randomly selected cell lines from 10 IgAN patients and 10 healthy controls and analyzed the binding of the secreted IgG to a synthetic IgA1 hinge-region peptide linked to BSA (HR-BSA) and a synthetic IgA1 hinge-region glycopeptide linked to BSA with 3 GalNAc residues (HR-GalNAc-BSA) at sites corresponding to the major epitopes of the Gal-deficient IgA1 myeloma protein (Thr228, Ser230, and Ser232) (25). The IgG from the cells derived from IgAN patients did not bind the HR-BSA but bound HR-GalNAc-BSA; moreover, the binding to HR-GalNAc-BSA was inhibited by HAA (78%) (Figure 2C). Thus, the IgG-secreting cells derived from the peripheral blood of patients with IgAN produced glycan-specific antibodies that recognize Gal-deficient IgA1 in a GalNAc-dependent manner. These IgG-producing cells were further subcloned to isolate single-cell clones producing antibodies specific for Gal-deficient IgA1. We randomly selected 3 cell lines from clones from patients with IgAN ($n = 16$) and 3 cell lines from clones from healthy controls ($n = 16$) and scaled up the cultures to obtain sufficient amounts of purified IgG for further characterization.

Glycan-specific IgG forms immune complexes with Gal-deficient IgA1. The ability of the glycan-specific antibodies to form immune complexes with Gal-deficient IgA1 was determined in vitro by incubation of the purified IgG proteins with a Gal-deficient IgA1 myeloma protein (Ale mono) at a 1:1 molar ratio. The reaction mixture was then fractionated by HPLC with the IgA1-IgG immune complexes being identified by cross-capture ELISA (25). Incubation of the Gal-deficient IgA1 with IgG produced by the cells derived from IgAN patients resulted in the production of greater amounts of immune complexes than were formed on incubation with IgG produced by cells derived from healthy controls (Figure 3A). Analysis of the size and composition of the immune complexes suggested that they were composed of 1 molecule of IgG bound to either 1 or 2 molecules of IgA1 (Figure 3A).

Analyses of the IGH, IGκ, and IGλ genes derived from patients with IgAN. The variable regions of *IGH* and *IG*κ or *IG*λ transcripts from single cells were amplified in 2 rounds of nested RT-PCR reactions using specific primers (33). The resultant amplicons were then purified and directly sequenced. The predicted aa sequences of the CDR3 of the variable region of the *IGH* gene (V_H genes) from the 7 IgAN patients analyzed differed significantly from the predicted sequences for the genes of the 6 healthy controls that were analyzed (Tables 1 and 2). One of the notable differences was that the 3′ end of V_H genes from cells of 6 IgAN patients included a sequence encoding YCSR/K, which represented an A to S substitution as compared with the sequence encoding YCAR that was identified in 5 of 6 controls (Table 1). In the 1 IgAN patient (subject 3081) who did not have the A to S substitution at this position, there was an R to T substitution at the next position (YCAT vs. YCAR). On dot-blot analysis, we found extensive binding of the IgG secreted by the cells from the IgAN patients to Gal-deficient IgA1 with 1 exception (IgG from the clone from subject 3081; Figure 3B). The IgG secreted by the cells from the healthy controls either did not bind to Gal-deficient IgA1 or exhibited significantly less binding, again with 1 exception (IgG from the clone from subject 3070 with the sequence YCAS) (Figure 3B). Densitometric analysis of these blots indicated that the IgG from IgAN patients exhibited greater binding to Gal-deficient IgA1 than did the IgG from healthy controls (Figure 3C; $P < 0.01$). Thus, the CDR3 of the V_H appears to play an important role in the binding of the glycan-specific IgG to the Gal-deficient IgA1, and the A to S substitution that we found in 6 of 7 patients with IgAN appears to be associated with enhanced binding.

The importance of the A to S substitution in the YCAR/K sequence of the CDR3 in the binding of IgG to Gal-deficient IgA1. For further analyses, we prepared recombinant human IgG (rIgG) using a single-cell PCR technique to clone the variable regions of the heavy- and light-chain genes of IgG from an IgG-secreting cell line derived from a patient with IgAN and from an IgG-secreting cell line derived from a healthy control. The corresponding PCR products for heavy and light chains were subcloned into Igγ and Igκ or λ expression vectors, respectively, to express rIgG1, also matching the original subclass of the identified antibodies. Western blot analysis demonstrated that the rIgG from the IgAN patient bound to Gal-deficient IgA1 myeloma protein (Ale poly) (Figure 4A), and this was confirmed by ELISA using Fab-IgA1. Furthermore, we purified the Fab fragment of the rIgG from an IgAN patient to confirm the role of the antigen-binding region in the interaction with Gal-deficient

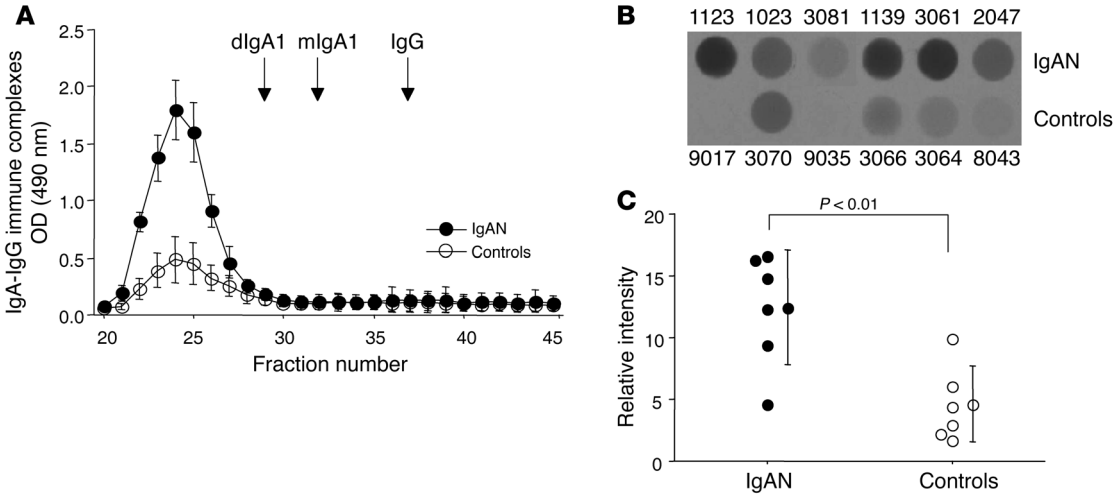

Figure 3

Characterization of immune-complex formation. (**A**) Size-exclusion chromatography and ELISA analysis of immune complexes formed in vitro with monomeric Gal-deficient IgA1 (50 μg) and glycan-specific IgG (50 μg) from 3 patients with IgAN (filled circles) or 3 healthy controls (open circles). IgG and monomeric (m) and dimeric (d) IgA1 standards were used to calibrate the column. Glycan-specific IgG from IgAN patients exhibited more binding to Gal-deficient IgA1 as compared with the binding of IgG from healthy controls. Immune complexes likely contained 1 or 2 molecules of IgA1 bound to 1 molecule of IgG. Data are shown as mean ± SD. (**B**) Dot-blot analysis showed that IgG secreted by cell lines from 5 of the 6 IgAN patients exhibited high binding to Gal-deficient IgA1; cell line no. 3081 from an IgAN patient and cells from 5 of the 6 healthy controls exhibited low binding. (**C**) Findings shown in Table 1 were confirmed by densitometrical analysis. $P < 0.01$; P values were generated using the 2-tailed Student's t test. Data are shown as individual values and mean ± SD. Experiments were repeated 3 times with similar results.

IgA1. ELISA data confirmed that the Fab fragment of rIgG bound to Fab-IgA1 in a fashion similar to that of the intact rIgG. Western blotting against the hinge region of native IgA1, desialylated IgA1, and dd-IgA1 myeloma proteins (Mce1) confirmed that the binding of the rIgG to IgA1 was increased after removal of sialic acid and Gal on the hinge region of IgA1 (Figure 4B).

To determine whether the aa substitution (A to S) in the CDR3 of the V_H domain of IgG from IgAN patients affects the binding to Gal-deficient IgA1, the V_H gene of the single-cell line from an IgAN patient (subject 1123) with the YCSR sequence was reverted to the counterpart found in most healthy controls (S to A) using an overlap PCR strategy (Supplemental Table 3) (34). Conversely, the CDR3 of the V_H gene of the single-cell line from a healthy control (subject 9017) encoding the YCAR sequence was mutated (A to S) to generate the sequence found in most of the IgAN patients. Both mutations were confirmed by sequencing after cloning into an IgG-expressing vector, as described above (Figure 4C). The rIgG was then purified and tested for binding to Gal-deficient IgA1 using Western blotting and ELISA. The S to A change in the CDR3 of the IgG of the IgAN patient reduced the binding of rIgG to Gal-deficient IgA1 by 72%. Conversely, the A to S substitution in CDR3 of the IgG of a healthy control increased binding to Gal-deficient IgA1 to 80% of that of the rIgG of the IgAN patient (Figure 4D). These data were confirmed by ELISA using Fab-IgA1 as the antigen.

Serum levels of IgG specific for Gal-deficient IgA1 are elevated in patients with IgAN. As we had found that patients with IgAN have higher levels of circulating IgG antibodies with specificity for Gal-deficient IgA1, we further evaluated the quantitative differences using what we believe is a novel dot-blot assay that we developed for this purpose (see Methods). We found that the IgAN patients (n = 60) had elevated levels of serum IgG specific for Gal-deficient IgA1 as compared with disease controls (n = 20) and healthy controls (n = 40) (Figure 5, A and B). The relative intensity values for the serum IgG antibodies from IgAN patients in both cohorts, disease controls, and healthy controls

Table 1

Comparison of the IgG heavy-chain CDR3 amino acid sequences from IgAN patients with those from healthy controls

Cells from IgAN patients	
Cell ID	**CDR3 (aa)**
1023	YC**S**RDLAAFCSGGNCHSVAIDFW
1123	YC**S**KVCRPWNYRRPYYYGMDVW
1125	YC**S**RDRYYCSGGAFDYW
1139	YC**S**RKTSYPPTVGEVRGTSYYYGMDVW
2047	YC**S**KTKFKGYSGFHYW
3061	YC**S**RDRYGLFDYW
3081	YCATGDYFGSGTYPIGAFDTW
Cells from healthy controls	
Cell ID	**CDR3 (aa)**
3066	YCARDLDLW
3070	YCA**S**EGHLDYGGNSDAFDIW
3064	YCARDVNITATEYYFDYW
8043	YCARGNDDYFDYW
9017	YCARVQRYDSTGYYPLGYLDLW
9035	YCAREWYSYLWDSSYYFDYW

The aa sequences of V_H CDR3 of IgG from 7 IgAN patients and 6 controls. There were notable differences, including a sequence YCSR/K, with a change of A to S (bold and underlined S; excluding subject 3081, who had sequence YCAT) in the CDR3 of heavy chain of IgG from IgAN patients compared with the YCAR sequence in the controls (except subject 3070; bold S).

Table 2
Repertoire and reactivity of antibodies from B cells of patients with IgAN and healthy controls

Ig	Heavy chain						Light chain					Reactivity with
cell ID	V	D	J	CDR3 (aa)	Length	pI	V	J	CDR3 (aa)	Length	pI	Gd-IgA1
Cells from patients with IgAN												
1023	1–46	2–15	4	YCSRDLAAFCSGGNCHSVAIDFW	20	5.61	κ2–29	κ1	CMQGIHLPPTVDVF	12	6.58	±
1123	3–23	1–7	6	YCSKVCRPWNYRRPYYYGMDVW	19	9.49	λ2–11	λ2	CCSYAGSYTSLF	10	13.00	+
1125	3–30	3–22	4	YCSRDRYYCSGGAFDYW	14	6.44	λ2–8	λ2	CSSYVGSNNSLF	10	13.00	+
1139	3–21	3–3	6	YCSRKTSYPPTVGEVRGTSYYYGMDVW	24	8.83	λ1–40	λ2	CQSYDSSLSGYVVF	12	13.00	+
2047	3–23	5–12	4	YCSKTKFKGYSGFHYW	13	9.84	κ1–5	κ1	CQQYNSYPWTF	9	13.00	+
3061	3–11	5–12	4	YCSRDRYGLFDYW	10	6.59	κ1–12	κ2	CQQANSFPPTGTF	11	13.00	+
3081	1–24	3–10	3	YCATGDYFGSGTYPIGAFDTW	18	13.00	κ1–39	κ1	CQQSYSTPRTF	9	9.25	–
Cells from healthy controls												
3064	4–4	3–9	4	YCARDVNITATEYYFDYW	15	4.10	λ1–50	λ2	CKAWDNSLNAHTVLQAVF	16	7.49	–
3066	3–7	–	2	YCARDLDLW	6	4.40	κ3–15	κ5	CQQYNNWPQTF	9	13.00	–
3070	4–59	4–23	3	YCASEGHLDYGGNSDAFDIW	17	3.92	κ1–39	κ5	CQQSYSTPPTF	9	13.00	±
8043	4–39	1–1	4	YCARGNDDYFDYW	10	4.10	κ3–20	κ2	CQQYGSSLYTF	9	13.00	–
9017	3–7	3–9	2	YCARVQRYDSTGYYPLGYLDLW	19	6.58	λ3–9	λ2	CQVWDSSSDVVF	10	13.00	–
9035	3–7	2–8	4	YCAREWYSYLWDSSYYFDYW	17	4.10	λ3–21	λ2	CQVWDSSSDHPF	10	4.39	–

V, variable; D, diversity; J, joint; +, high reactivity; ±, medium reactivity; –, no reactivity.

were 33.2 ± 14.6, 9.9 ± 3.9, and 9.0 ± 6.8, respectively (Figure 5B; $P < 0.0001$). To test the reproducibility of this assay, the same serum samples were reanalyzed twice, and the difference between the experiments was 3.5% ± 2.3%. Notably, 54 of the 60 patients with IgAN had mean binding values higher than the 90th percentile of those for healthy controls. A receiver operating characteristic curve (ROC) analysis indicated the area under the curve was 0.9644 (Figure 5C; $P < 0.0001$); when the level of serum IgG specific for Gal-deficient IgA1 specificity reached 95.0%, the corresponding sensitivity was 88.3%. Furthermore, for 20 IgAN patients with urine and blood samples collected within 30 days of renal biopsy (contemporaneous samples), we assessed possible correlations among clinical and laboratory findings. The results of these analyses showed that the intensity of binding of IgG to Gal-deficient IgA1 as determined by the dot-blot analysis correlated with proteinuria (expressed as urinary protein/urinary creatinine [UP/Cr] ratio; Figure 5D; $P < 0.0001$) as well as with urinary IgA-IgG immune complexes (expressed relative to Cr concentration; Figure 5E; $P = 0.0082$).

Discussion

The results of our studies provide evidence that sera and culture supernatants of EBV-immortalized peripheral B cells of patients with IgAN contain elevated levels of IgG antibodies specific for the Gal-deficient hinge-region *O*-glycans of IgA1. Comparative evolutionary studies of this structurally unique hinge region of IgA in many species indicate that IgA1 in humans, chimpanzees, and gorillas was generated by an insertion of a gene segment encoding an additional 13 amino acids into phylogenetically older IgA that structurally resembles human IgA2 (35, 36). The origin of this insertion remains obscure: there is no pronounced sequence homology to any other glycoprotein, and the hinge region of human IgA1 is the only known substrate for the family of enzymes, bacterial IgA-specific proteases, that cleave human IgA1 into Fab and Fc fragments with functionally important biological consequences (37). Although the structural and functional impact conferred by the hinge-region insertion into hominoid primate IgA1 remains elusive, it is obvious that alterations in the associated glycan moieties are of paramount significance in IgAN (21, 24, 25). Our data indicate that GalNAc plays an important role in the interaction between IgG and Gal-deficient IgA1. GalNAc appears to act as an epitope in itself, as indicated by additional experiments that assessed binding of this IgG antibody to GalNAc- or *N*-acetylglucosamine–Sepharose (GlcNAc-Sepharose), although it is possible that differences in glycosylation may affect the hinge-region protein backbone conformation and contribute to the epitope configuration. Thus, these results confirmed and extended our previous report (21) indicating that GalNAc-Sepharose inhibited reformation of dissociated IgA1-containing immune complexes isolated from the circulation of patients with IgAN.

The development of a dot-blot assay using Gal-deficient IgA1 as an antigen and GalNAc-specific rIgG from an IgAN patient as a standard permitted accurate analysis of the levels of glycan-specific IgG in the sera with high specificity and sensitivity. Notably, our results showed that serum levels of this IgG that is specific for Gal-deficient IgA1 correlated with the clinical parameter of proteinuria as well as with levels of urinary IgA1-IgG immune complexes, suggesting that the levels of these antibodies may represent a marker of disease activity and thus may be useful in assessing response to treatment.

The finding that the binding of the glycan-specific IgG from patients with IgAN to Gal-deficient IgA1 greatly favored the formation of immune complexes suggests that these glycan-specific antibodies may play a role in the pathogenesis of IgAN. It has been shown previously that IgA1-containing immune complexes from patients with IgAN bind to mesangial cells with higher affinity than does uncomplexed IgA1 (23) and that IgA1-IgG immune complexes stimulate proliferation of mesangial cells and increase secretion of cytokines/chemokines and extracellular matrix proteins, mimicking the findings in IgAN renal biopsies (24, 25). Notably, uncomplexed Gal-deficient IgA1 does not seem to affect cellular proliferation (24, 25).

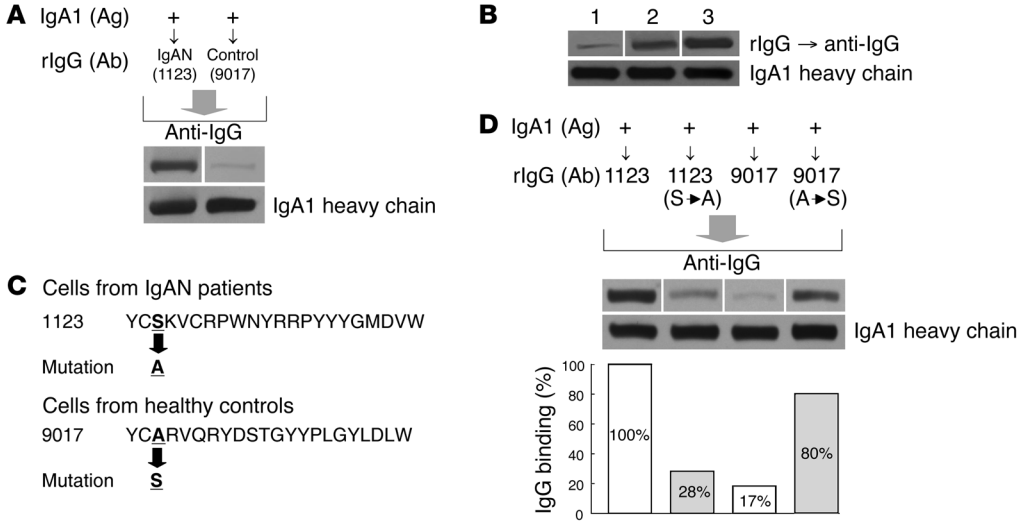

Figure 4

Importance of the A to S substitution in YCAR/K sequence of CDR3 in the binding of IgG to Gal-deficient IgA1. (**A**) Western blot analysis using Gal-deficient IgA1 (Ale poly) as antigen demonstrated binding of rIgG cloned from an IgAN patient (subject 1123) but only marginal binding of rIgG from a healthy control (subject 9017). (**B**) The reduced Gal-deficient IgA1 (Mce1) (lane 1); enzymatically desialylated Gal-deficient IgA1 (lane 2); and desialylated and degalactosylated Gal-deficient IgA1 (lane 3) were incubated with rIgG after SDS-PAGE/Western blotting. Removal of sialic acid and Gal in the IgA1 hinge region increased the binding, suggesting that the rIgG bound specifically to GalNAc. (**C**) The aa sequence (YCSK) in the CDR3 of V_H of IgG from an IgAN patient (subject 1123) was reverted to the healthy control germline counterpart sequence (YCAK) using an overlap PCR strategy. Conversely, the CDR3 of IgG from a healthy control (subject 9017) was mutated to generate YCSR. (**D**) After the S to A substitution was introduced in CDR3 of V_H of IgG of the cells from an IgAN patient (subject 1123), rIgG binding to Gal-deficient IgA1 was reduced by 72%. Conversely, the A to S substitution in CDR3 of IgG of the cells from a healthy control (subject 9017) increased binding to Gal-deficient IgA1. Anti-human IgA (heavy-chain specific) Western blotting was used as load control. Results were evaluated densitometrically. Representative results from 2 experiments are shown in **A**–**D**; lanes were run on the same gel but were noncontiguous.

In an experimental rat model of IgAN, simultaneous administration of IgA and IgG has been shown to increase proteinuria via a complement-dependent mechanism (38). A pathogenic role of IgG in renal deposits is supported by the observation that mesangial IgG deposition in the presence of normal renal function is a risk factor for decreased renal survival in IgAN patients (39). In our patients who were sampled within 30 days of renal biopsy, there was, however, no apparent correlation between serum levels of IgG specific for Gal-deficient IgA1 and the quantity of glomerular IgG deposits as determined by renal pathologists.

We show that the glycan-specific IgG antibodies bind to Gal-deficient IgA1 and form immune complexes, which is consistent with earlier reports (24, 25). It has been shown previously that these circulatory immune complexes are not effectively catabolized by the liver and are deposited in the glomerular mesangial area due to their large size rather than through binding to an intrinsic glomerular antigen. Sedivá et al. (40) assessed the expression of carbohydrate-binding site(s) in the human kidney. The authors did not find GalNAc-containing epitopes in the mesangium in any of the tested samples, suggesting that the glycan-specific IgG itself will not be directed to mesangium. Consequently, both Gal-deficient IgA1 and glycan-specific IgG are necessary for induction of IgAN. Direct evidence supporting the pathogenic role of IgA1-IgG immune complexes came from experiments using cultured human mesangial cells (24, 25). The results of our ongoing studies suggest that anti-glycan IgG antibodies from IgAN patients, but not IgG from healthy controls without anti-glycan specificity, form IgA1-IgG complexes that stimulate proliferation of cultured human mesangial cells. Furthermore, Gal-deficient IgA1 or anti-glycan IgG alone does not exhibit these stimulatory activities (J. Novak et al., unpublished observations).

If the IgG does play a direct role in eliciting pathogenic changes in the mesangium, one would expect that IgG codeposits would be detectable in biopsy specimens. There are, however, considerable differences in the literature in terms of the estimated frequency and degree of IgG deposition in patients with IgAN, and in the clinic, it is not unusual for pathology reports to indicate that IgG deposition is absent or minimal. Reports in the literature regarding the frequency and degree of IgG deposition in patients with IgAN are based on pathology reports, and these typically suggest the presence of IgG codeposits in about 60% of biopsies (41–43). It is possible therefore that the reported low frequencies reflect the relative insensitivity of the assays used in the clinical laboratories and the variability reflects the different protocols and/or antibodies used for immunohistochemical analysis in different laboratories. Our experience suggests that this may be the case, as confocal microscopic evaluation of biopsy specimens from 7 IgAN patients indicated that IgG could be detected by immunofluorescent staining in the glomeruli of the 6 specimens that contained glomeruli and that IgG-IgA complexes were detectable in the tubules of the specimen that did not contain glomeruli. In contrast, the pathology reports stated that although all of the samples had IgA, 2 of the samples had no IgG and 2 samples, only trace amounts. In the 3 samples that were reported as being positive for IgG, the intensity was described as 1+. Thus, IgG codeposits are likely more frequent than reported in the literature or than would be expected based on pathology reports (L. Novak et al, unpublished observations). This observation, as well as the question as to whether the timing

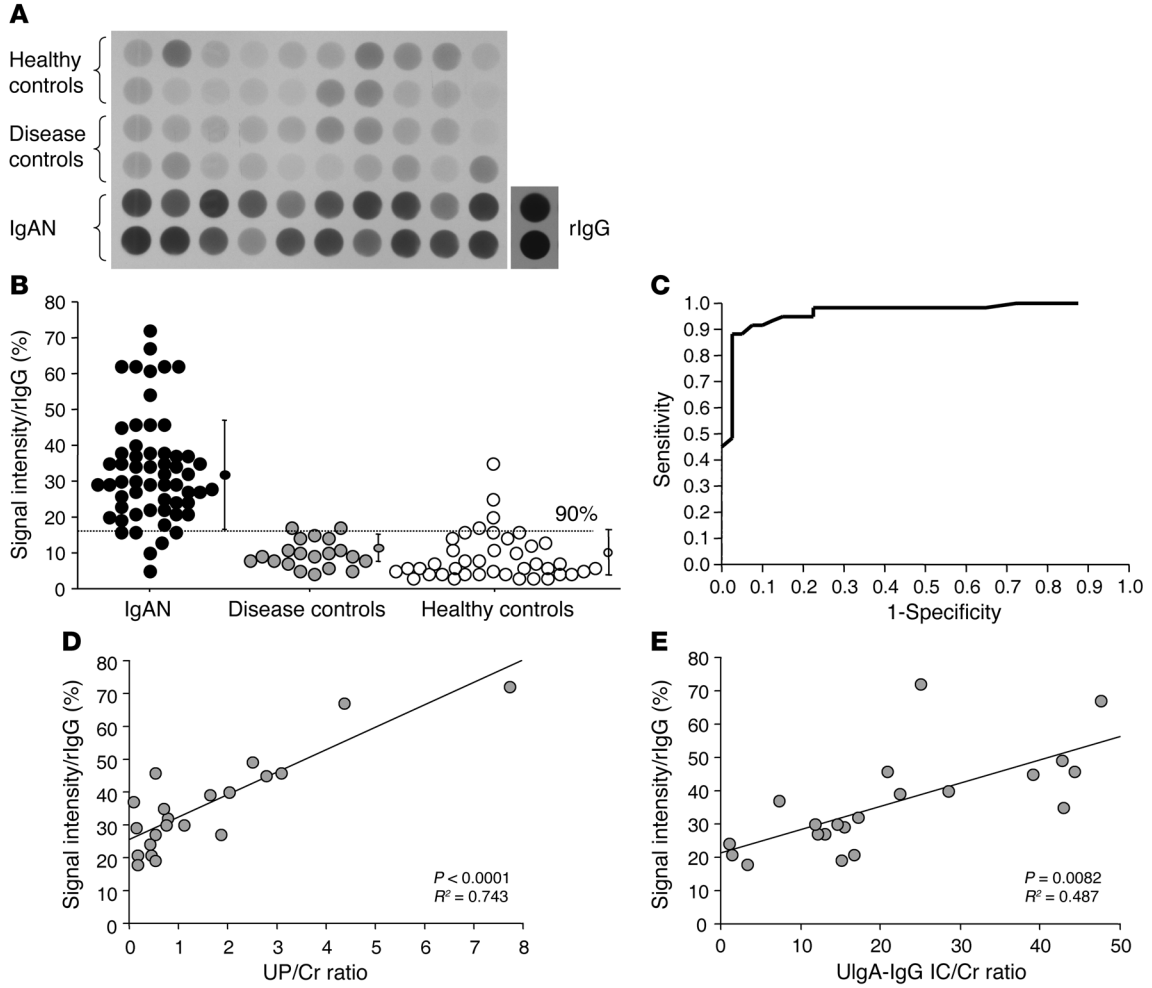

Figure 5

Serum levels of IgG specific for Gal-deficient IgA1 are elevated in patients with IgAN. (**A**) Gal-deficient IgA1 (Ale) placed in 96-well plates with PVDF membranes was incubated with normalized concentrations of serum IgG from IgAN patients, disease controls, and healthy controls; a representative example from 3 experiments is shown (20 samples from each group). The rIgG from an IgAN patient served as a positive control. Serum IgG from IgAN patients bound more to Gal-deficient IgA1 compared with the IgG from disease controls or healthy controls. (**B**) The intensity of signal in each well was measured by densitometry; the intensity of rIgG bound to Gal-deficient IgA was assigned a value of 100%. Serum IgG from IgAN patients has significantly higher reactivity to Gal-deficient IgA1 compared with that from healthy ($P < 0.0001$) and disease controls ($P < 0.0001$). Serum IgG from 54 of the 60 patients with IgAN showed values greater than the 90th percentile of the values for healthy controls. Wilcoxon's rank-sum test was used for 2-sample comparison. Data are shown as individual values and the mean ± SD. (**C**) ROC for serum IgG binding to Gal-deficient IgA1. The area under the curve is 0.9644. These data indicate a sensitivity of 88.3% and a specificity of 95.0% ($P < 0.0001$; 95% CI, 0.928-1.00). The value of specificity is plotted as 1-specificity on the *x* axis. (**D**) The intensity of IgG binding to Gal-deficient IgA1 correlated with the UP/Cr ratio ($P < 0.0001$) as well as with urinary IgA-IgG immune complexes (**E**) ($P = 0.0082$) in contemporaneously collected urine samples. UIgA-IgG IC/Cr, urinary excretion of IgA-IgG immune complexes/creatinine ratio.

of the biopsy in terms of the state of disease progression affects the finding of IgG codeposits, requires further study.

Although the origin of the glycan-specific antibodies remains unclear, some viruses and bacteria express GalNAc-containing molecules on their surface structures (8). We speculate that in patients with IgAN, an infection with one of these microorganisms induces production of glycan-specific antibodies that cross-react with Gal-deficient IgA1. This hypothesis is supported by the clinical observation that in patients with IgAN, urinary abnormalities are frequently exacerbated during upper–respiratory tract infections (synpharyngitic hematuria) (44). Furthermore, higher levels of circulatory IgA1-containing immune complexes have been observed during episodes of increased clinical activity marked by macroscopic hematuria (7, 20, 24). While the IgG antibodies against Gal-deficient IgA1 appear to be predominantly glycan-specific, it is possible that serum polyclonal IgG may contain additional types of antibodies generated by the epitope-spreading process described in many autoimmune diseases (45). Furthermore, we have reported previously that not only IgG but also IgA1 in the sera of IgAN patients can bind to Gal-deficient IgA1 (21). Future studies are needed, perhaps even using IgA1-secreting cell lines (19), to determine the role of IgA1 antibodies against Gal-deficient IgA1 in the pathology of IgAN and to investigate the possibility that such antibodies also may be aberrantly glycosylated.

Analyses of the *IGH* gene sequences encoding antibodies specific for Gal-deficient IgA1 from IgAN patients indicated that these *Ig* genes have been positively selected during active immune responses because all the V_H gene sequences have mutations compared with the corresponding germline V_H genes (46, 47). Although there is no specific selection of the V_H, diversity region of the *IGH* gene (D_H), or joint region of *IGH* gene (J_H) gene usage, 6 of the 7 antibodies specific for Gal-deficient IgA1 share the same A to S substitution within the CDR3 of the IgH (CDR-H3) (the YCSR/K motif). Normally, the CDR-H3 is located in the center of the antigen-binding sites and is the main determinant of antibody specificity (48). The specific selection of the YCSR/K motif within these IgAN-specific antibodies suggests that this particular region is directly involved in binding Gal-deficient IgA1. Indeed, changing the S residue back to A residue dramatically reduced the capacity of the IgAN antibody (subject 1123) to bind the Gal-deficient IgA1; conversely, artificially changing the A to S in a control antibody (subject 9017) strongly enhanced its binding to the Gal-deficient IgA1. These results provide what we believe is the first information regarding the molecular signature of IgG specific for Gal-deficient IgA1 in IgAN patients. Currently, it is not known whether this change originated from genetic variation or somatic mutation during active immune response (49, 50). Further analysis of the generation and selection of antibodies with this signature during the course of IgAN will provide new insights into its pathogenesis.

Methods

Human subjects. Peripheral blood was collected from a total of 60 patients with biopsy-proven IgAN (mean age, 34.8 ± 12.5 years; serum creatinine, 1.3 ± 0.6 mg/dl; UP/Cr ratio, 1.31 ± 1.60), from 40 healthy controls (mean age, 38.0 ± 16.2 years; serum creatinine, 0.9 ± 0.2 mg/dl; UP/Cr ratio, 0.06 ± 0.06), and from 20 disease controls (patients with biopsy-proven lupus nephritis, membranous nephritis, and minimal change nephrotic syndrome; mean age, 35.0 ± 11.4 years; serum creatinine, 1.1 ± 0.4 mg/dl; UP/Cr ratio, 1.56 ± 1.93) (Supplemental Table 4). The IgAN patients included 16 white males and 9 white females, 1 African-American male and 2 African-American females, and 12 Japanese males and 20 Japanese females. The healthy control group consisted of 12 white males and 12 white females, 2 African-American males and 4 African-American females, and 4 Japanese males and 6 Japanese females. All healthy controls had normal UP/Cr ratio or dipstick test for protein, and none exhibited microscopic hematuria. Disease controls consisted of a group of 5 white males and 1 white female and 1 African-American female, and 7 Japanese males and 6 Japanese females. We determined the levels of IgA, Gal-deficient IgA1, and IgG in the serum samples from the 60 IgAN, 20 disease controls, and 40 healthy control subjects by capture ELISA. For 20 of 60 patients with IgAN, urine and blood samples were collected within 30 days of renal biopsy (contemporaneous samples). The Institutional Review Boards at the University of Alabama at Birmingham, the University of Tennessee Health Sciences Center, and Juntendo University School of Medicine approved this study. Written informed consent was obtained from all adults and from a parent or legally authorized representative for all children; children age 8 years or older provided signed assent.

Isolation of PBMCs, transformation with EBV, and cloning of IgG-secreting cell lines. PBMCs from patients with IgAN and healthy controls were isolated from heparinized peripheral blood by Ficoll-Hypaque density gradient centrifugation. The B cell fraction was enriched from the PBMCs by removal of adherent cells through incubation in a plastic tissue-culture flask for 1 hour at 37°C and removal of T cells by CD3 (PanT) Dynabeads, according to the manufacturer's instructions (Dynal; Invitrogen). PBMCs from 16 randomly selected IgAN patients (10 white males and 6 white females; 13 subjects had proteinuria or microscopic hematuria at the time of study) and 16 randomly selected white healthy controls (6 white males and 10 white females) were then immortalized with EBV (19, 51) in the Center for Clinical and Translational Science of the University of Alabama at Birmingham. To establish cell lines from the initial EBV-immortalized PBMCs from patients with IgAN and healthy controls, we subcloned IgG-secreting cells by limiting dilution (using 96-well plates seeded with 5 to 10 cells per well) in RPMI 1640 supplemented with L-glutamine, 20% FCS, penicillin, and streptomycin (19). After several rounds of cloning and screening, IgG-producing cell lines were generated from all 16 IgAN patients and all 16 healthy controls.

Measurement of Ig and immune-complex levels. The isotypes of the Igs secreted by the immortalized cells were determined by capture ELISA (21, 31). ELISA plates were coated with 1 μg/ml of the $F(ab')_2$ fragment of goat IgG specific for human IgA, IgG, or IgM (Jackson ImmunoResearch Laboratories Inc.). The captured Igs were then detected with a biotin-labeled $F(ab')_2$ fragment of goat IgG anti-human IgA, IgG, or IgM antibody (BioSource). Avidin–horseradish peroxidase conjugate (ExtrAvidin; Sigma-Aldrich) and the peroxidase chromogenic substrate *o*-phenylenediamine–H_2O_2 (Sigma-Aldrich) were then added. The color reaction was stopped with 1 M sulfuric acid, and the absorbance at 490 nm was measured using an EL312 BioKinetics Microplate Reader (BioTek). Standard curves for Igs were generated from a pool of normal human sera calibrated for all Ig isotypes (Binding Site). The results were calculated using a DeltaSoft III computer program (BioMetallics). Urinary IgA-IgG immune complexes were measured using cross-capture ELISA (52).

Myeloma proteins. The IgA1 myeloma proteins that were isolated from plasma of patients with multiple myeloma are listed in Supplemental Table 1 together with their molecular characteristics (31). In brief, plasma samples were precipitated with ammonium sulfate (50% saturation). The precipitate was then dissolved in and dialyzed against 10 mM sodium phosphate buffer (pH 7.0) prior to fractionation by ion-exchange chromatography on DEAE-cellulose, followed by affinity chromatography using Jacalin-agarose to capture IgA1 (Sigma-Aldrich) (21). The final purification step was size-exclusion chromatography on columns of Sephadex G-200 or Ultrogel AcA 22 (Amersham Biosciences). As the IgA myeloma proteins can be contaminated with IgG, the purified protein was subjected to affinity chromatography using staphylococcal protein G immobilized on agarose (Sigma-Aldrich). The purity of the IgA1 preparations was assessed by SDS-PAGE and Western blotting using an IgA1-specific monoclonal antibody (21). The molecular form of the IgA1 proteins was assessed by size-exclusion chromatography, SDS-PAGE under nonreducing conditions, and Western blots developed with anti-IgA antibody.

ELISA characterization of antigen-specific IgG antibodies. The binding of serum IgG from IgAN patients and healthy controls, as well as IgG secreted by EBV-immortalized cells from the same subjects, was analyzed by ELISA using a panel of antigens: dd-IgA1, Fab-IgA1 generated using an IgA-specific protease from *Haemophilus influenzae* HK50, HR-BSA, and HR-GalNAc-BSA. HR-GalNAc was synthesized by Bachem (asterisks mark the sites with GalNAc): V-P-S-T-P-P-*T-P-*S-P-*S-T-P-P-T-P-S-P-S- C-NH_2. The hinge-region peptide was the same peptide but with no GalNAc. Both preparations were cross-linked to BSA.

For ELISA, flat-bottom 96-well plates (MaxiSorp; Nunc) were coated with 1 μg/ml solution of the above-mentioned antigens. Serum or culture supernatant samples diluted in PBS were added to each well. The amount of total IgG used for the analyses was normalized in all samples. The captured IgG were detected with a biotin-labeled $F(ab')_2$ fragment of goat IgG anti-human IgG antibody (BioSource; Invitrogen). Avidin–horseradish peroxidase conjugate (ExtrAvidin; Sigma-Aldrich) was then added, and the reaction was developed as described before (19).

SDS-PAGE and Western blotting. Serum and culture supernatants were separated by SDS-PAGE under reducing conditions using 4%–20% gradient slab gels (Bio-Rad). The amounts of protein loaded were adjusted to achieve equivalent amounts of IgA protein in each lane. The gels were blotted onto PVDF membranes and incubated with antibody specific for IgA heavy chains (Vector Laboratories) or a biotin-labeled HAA lectin. HAA reacts with terminal GalNAc but not with sialylated GalNAc or GalNAc-Gal disaccharide. Gal-deficient IgA1 myeloma proteins (Mce or Ale poly), after separation by SDS-PAGE under reducing conditions and electroblotting onto PVDF membranes, served as antigens for analysis of glycan-specific IgG. The bound IgG was detected with IgG-specific antibody, and the visualization of positive bands was accomplished by subsequent incubation of the membrane with avidin-peroxidase conjugate, followed by enhanced chemiluminescence detection (Pierce; Thermo Scientific) (30–32).

HAA inhibition. To inhibit IgG binding to Gal-deficient IgA1 (Mce) myeloma protein or HR-GalNAc-BSA, 20 μg/ml unlabeled HAA was applied to PVDF membrane after electroblotting of IgA1 or to the wells of ELISA plates after coating with IgA1 protein.

Immune-complex formation in vitro. IgG was isolated from cell-culture supernatants of the IgG-secreting cell lines derived from patients with IgAN and healthy controls by protein G affinity chromatography (GE Healthcare). These cell lines were subcloned by limiting dilution, and clones secreting glycan-specific IgG (binding to Gal-deficient IgA1) were selected. Immune complexes were formed in vitro by mixing 50 μg Gal-deficient IgA1 (Ale mono) and 50 μg purified glycan-specific IgG and incubating the mixture overnight at 4°C. The formed complexes were fractionated by HPLC on a calibrated TSK 3000 column (Tosoh Bioscience), and 0.25 ml fractions were analyzed for IgA1-IgG immune complexes using cross-capture ELISA (25).

Cloning of IGH, IGκ, and IGλ genes. Single-cell reverse-transcription PCR was used to amplify the V(D)J regions for *IGH*, *IG*κ, and *IG*λ genes (33). Reverse transcription and first-round PCR were performed with OneStep RT-PCR Kit (QIAGEN) under these conditions: 50°C, 30 minutes; 94°C, 15 minutes; 94°C, 20 seconds; 55°C, 30 seconds; 72°C, 1 minute for 50 cycles; 72°C, 10 minutes; and stop at 4°C. Second-round PCR was performed with rTaq DNA Polymerase (Invitrogen) under these conditions: 94°C, 3 minutes; 94°C, 20 seconds; 57°C (IgH/Igκ) or 60°C (Igλ), 30 seconds; 72°C, 45 seconds for 50 cycles; 72°C, 5 minutes; and stop at 4°C. One microliter of cDNA from first-round PCR was used as the template for the second-round PCR. The average single-cell RT-PCR efficiency was 38.4%. Positive PCR products were purified (QIAquick; QIAGEN) and sequenced. The resultant Ig gene sequences were analyzed with the IgBLAST program to determine the potential V_H, D_H, and J_H germline gene usage and mutation analysis (http://www.ncbi.nlm.nih.gov/igblast/). Restriction enzyme digestion sites were introduced in the second round of single-cell RT-PCR. Digested IgH, Igκ, and Igλ PCR products were purified using QIAquick PCR purification kit (QIAGEN) and directly cloned into specific expression vectors containing human Igγ1, Igκ, or Igλ constant regions. Plasmids were sequenced to confirm clones with inserts identical to that of the original PCR products. The pI values and CDR3 junction analysis were determined by IMGT/V-QUEST (http://www.imgt.org/IMGT_vquest/vquest). The corresponding DNA sequences were deposited to GenBank (accession numbers FJ746335–FJ746360).

V_H CDR3 site-specific mutagenesis. Site-directed mutagenesis was performed by 2-step PCR to generate amplicons with mutated (IgAN patient 1123) or unmutated (healthy control 9017) V_H genes (34). Primers used in PCR reverted the substitution (S to A) in the IgAN clone or mutated (A to S) the sequence in the clone from the healthy control (Supplemental Table 3). The first PCR (PCR1) forward primer was V_H specific and contained an *AgeI* restriction site. The PCR2 reverse primer was J_H specific and contained the *SalI* restriction site. PCR products 1 and 2 were hybridized via the homologous region in the subsequent overlap PCR using the same 5′-*AgeI* V_H-specific forward primer and the 3′ *SalI* J_H-specific reverse primer and generated the complete *VDJ* sequence with desired mutations. Corresponding clones were sequenced and cloned into the IgG expression vector for production of rIgG.

rIgG antibody production. Human embryonic kidney cells (293H) were cultured in DMEM supplemented with 10% FBS (Ultra Low Bovine Ig content; Gibco, Invitrogen) and cotransfected with 10 μg plasmid DNA constructs encoding IgH and IgL chains by polyethyleneimine (Sigma-Aldrich) precipitation. After 16-hour transfection, the cell-culture medium was replaced with fresh medium. Supernatants with secreted IgG were collected after 7 days.

Fab purification of rIgG. The Fab fragment of rIgG from an IgAN patient was purified using the Pierce Fab Preparation Kit (Thermo Scientific).

Dot-blot analysis. Gal-deficient IgA1 (Ale poly; 0.5 μg per well) was placed into the wells of a 96-well plate with PVDF membrane (MultiScreen$_{HTS}$ IP Filer Plate; Millipore) and blocked with SuperBlock (Pierce; Thermo Scientific). Serum or cell-culture supernatants (normalized to 0.5 μg IgG in each sample) were added and incubated overnight at 4°C. As a positive control, 0.5 μg of rIgG from an IgAN patient was used. The binding was detected with IgG-specific antibody, followed by subsequent incubation of the membrane with avidin-peroxidase conjugate, and the reaction was visualized using enhanced chemiluminescence (Pierce; Thermo Scientific), as described above for Western blotting. Results were evaluated densitometrically. The intensity of rIgG binding to Gal-deficient IgA was assigned a value of 100%.

Statistics. Correlations between different parameters were analyzed by 2-tailed Student's *t* test or by regression analysis. ANOVA was used to determine differences in the characteristics among multiple groups. Nonparametric methods, such as Spearman's rank correlation and Wilcoxon's rank-sum test were used for the correlation and 2-sample comparisons, respectively. Data were expressed as mean ± SD or median values. $P < 0.05$ was considered significant. These statistical analyses were performed with StatView 5.0 software (Abacus Concepts). The ROC for Gal-deficient IgA1-specific IgG levels in patients and controls was constructed using GraphPad Prism, version 4.00 for Windows (GraphPad Software).

Acknowledgments

This work was supported by NIH grants DK078244, DK080301, DK071802, DK082753, DK075868, DK061525, DK077279, and DK064400 and by the Center for Clinical and Translational Sciences of the University of Alabama at Birmingham (1UL1RR025777-01), the University of Tennessee Health Sciences Center (M01 RR00211), and research project VZMSM002162081 from the Ministry of Education, Youth, and Sports of the Czech Republic. We thank Richard Novak (University of California, Berkeley, Berkeley, California, USA) for his advice on primer design for mutagenesis and Lea Novak (University of Alabama at Birmingham) for staining and evaluation of renal biopsy specimens by confocal microscopy. We thank Catherine V. Barker, Susan Y. Woodford, and Nephrology Associates of Lexington, PSC, Lexington, Kentucky, USA, for assistance with the collection of blood samples and management of clinical data. The authors appreciate the critical reading of the manuscript by Fiona Hunter.

Received for publication January 5, 2009, and accepted in revised form April 15, 2009.

Address correspondence to: Jan Novak, Department of Microbiology, University of Alabama at Birmingham, 845 19th Street South, BBRB 734, Birmingham, Alabama 35294, USA. Phone: (205) 934-4480; Fax: (205) 934-3894; E-mail: jannovak@uab.edu.

1. Berger, J., and Hinglais, N. 1968. Les depots intercapillaires d'IgA-IgG (Intercapillary deposits of IgA-IgG). *J. Urol. Nephrol. (Paris).* **74**:694–695.
2. D'Amico, G. 2000. Natural history of idiopathic IgA nephropathy: role of clinical and histological prognostic factors. *Am. J. Kidney Dis.* **36**:227–237.
3. Julian, B.A., and Novak, J. 2004. IgA nephropathy: an update. *Curr. Opin. Nephrol. Hypertens.* **13**:171–179.
4. Conley, M.E., Cooper, M.D., and Michael, A.F. 1980. Selective deposition of immunoglobulin A1 in immunoglobulin A nephropathy, anaphylactoid purpura nephritis, and systemic lupus erythematosus. *J. Clin. Invest.* **66**:1432–1436.
5. Tomino, Y., Endoh, M., Nomoto, Y., and Sakai, H. 1981. Immunoglobulin A1 in IgA nephropathy. *N. Engl. J. Med.* **305**:1159–1160.
6. Russell, M.W., Mestecky, J., Julian, B.A., and Galla, J.H. 1986. IgA-associated renal diseases: Antibodies to environmental antigens in sera and deposition of immunoglobulins and antigens in glomeruli. *J. Clin. Immunol.* **6**:74–86.
7. Coppo, R., and Amore, A. 2004. Aberrant glycosylation in IgA nephropathy (IgAN). *Kidney Int.* **65**:1544–1547.
8. Novak, J., Julian, B.A., Tomana, M., and Mestecky, J. 2008. IgA glycosylation and IgA immune complexes in the pathogenesis of IgA nephropathy. *Semin. Nephrol.* **28**:78–87.
9. Barratt, J., Smith, A.C., and Feehally, J. 2007. The pathogenic role of IgA1 *O*-linked glycosylation in the pathogenesis of IgA nephropathy. *Nephrology (Carlton).* **12**:275–284.
10. Mestecky, J., et al. 1993. Defective galactosylation and clearance of IgA1 molecules as a possible etiopathogenic factor in IgA nephropathy. *Contrib. Nephrol.* **104**:172–182.
11. Allen, A.C., et al. 2001. Mesangial IgA1 in IgA nephropathy exhibits aberrant *O*-glycosylation: Observations in three patients. *Kidney Int.* **60**:969–973.
12. Hiki, Y., et al. 2001. Mass spectrometry proves under-*O*-glycosylation of glomerular IgA1 in IgA nephropathy. *Kidney Int.* **59**:1077–1085.
13. Tomana, M., et al. 1997. Galactose-deficient IgA1 in sera of IgA nephropathy patients is present in complexes with IgG. *Kidney Int.* **52**:509–516.
14. Allen, A.C., Harper, S.J., and Feehally, J. 1995. Galactosylation of *N*- and *O*-linked carbohydrate moieties of IgA1 and IgG in IgA nephropathy. *Clin. Exp. Immunol.* **100**:470–474.
15. Mattu, T.S., et al. 1998. The glycosylation and structure of human serum IgA1, Fab, and Fc regions and the role of *N*-glycosylation on Fcα receptor interactions. *J. Biol. Chem.* **273**:2260–2272.
16. Allen, A.C., Topham, P.S., Harper, S.J., and Feehally, J. 1997. Leucocyte β1,3 galactosyltransferase activity in IgA nephropathy. *Nephrol. Dial. Transplant.* **12**:701–706.
17. Qin, W., et al. 2005. Peripheral B lymphocyte β1,3-galactosyltransferase and chaperone expression in immunoglobulin A nephropathy. *J. Intern. Med.* **258**:467–477.
18. Buck, K.S., et al. 2008. B-cell *O*-galactosyltransferase activity, and expression of *O*-glycosylation genes in bone marrow in IgA nephropathy. *Kidney Int.* **73**:1128–1136.
19. Suzuki, H., et al. 2008. IgA1-secreting cell lines from patients with IgA nephropathy produce aberrantly glycosylated IgA1. *J. Clin. Invest.* **118**:629–639.
20. Coppo, R., et al. 1982. Circulating immune complexes containing IgA, IgG and IgM in patients with primary IgA nephropathy and with Henoch-Schönlein nephritis. Correlation with clinical and histologic signs of activity. *Clin. Nephrol.* **18**:230–239.
21. Tomana, M., et al. 1999. Circulating immune complexes in IgA nephropathy consist of IgA1 with galactose-deficient hinge region and antiglycan antibodies. *J. Clin. Invest.* **104**:73–81.
22. Mestecky, J., et al. 2008. The role of aberrant glycosylation of IgA1 molecules in the pathogenesis of IgA nephropathy. *Kidney Blood Press. Res.* **31**:29–37.
23. Novak, J., et al. 2002. Interactions of human mesangial cells with IgA and IgA-containing circulating immune complexes. *Kidney Int.* **62**:465–475.
24. Novak, J., et al. 2005. IgA1-containing immune complexes in IgA nephropathy differentially affect proliferation of mesangial cells. *Kidney Int.* **67**:504–513.
25. Novak, J., et al. 2007. IgA nephropathy and Henoch-Schoenlein purpura nephritis: aberrant glycosylation of IgA1, formation of IgA1-containing immune complexes, and activation of mesangial cells. *Contrib. Nephrol.* **157**:134–138.
26. Moura, I.C., et al. 2004. Glycosylation and size of IgA1 are essential for interaction with mesangial transferrin receptor in IgA nephropathy. *J. Am. Soc. Nephrol.* **15**:622–634.
27. Berger, J. 1988. Recurrence of IgA nephropathy in renal allografts. *Am. J. Kidney Dis.* **12**:371–372.
28. Schena, F.P., et al. 1989. Increased serum levels of IgA1-IgG immune complexes and anti-$F(ab')_2$ antibodies in patients with primary IgA nephropathy. *Clin. Exp. Immunol.* **77**:15–20.
29. Jackson, S., Montgomery, R.I., Julian, B.A., Galla, J.H., and Czerkinsky, C. 1987. Aberrant synthesis of antibodies directed at the Fab of IgA in patients with IgA nephropathies. *Clin. Immunol. Immunopath.* **45**:208–213.
30. Suzuki, H., et al. 2007. IgA nephropathy: characterization of IgG antibodies specific for galactose-deficient IgA1. *Contrib. Nephrol.* **157**:129–133.
31. Moore, J.S., et al. 2007. Reactivities of *N*-acetylgalactosamine-specific lectins with human IgA1 proteins. *Mol. Immunol.* **44**:2598–2604.
32. Moldoveanu, Z., et al. 2007. Patients with IgA nephropathy have increased serum galactose-deficient IgA1 levels. *Kidney Int.* **71**:1148–1154.
33. Wardemann, H., et al. 2003. Predominant autoantibody production by early human B cell precursors. *Science.* **301**:1374–1377.
34. Tiller, T., et al. 2008. Efficient generation of monoclonal antibodies from single human B cells by single cell RT-PCR and expression vector cloning. *J. Immunol. Methods.* **329**:112–124.
35. Sumiyama, K., Saitou, N., and Ueda, S. 2002. Adaptive evolution of the IgA hinge region in primates. *Mol. Biol. Evol.* **19**:1093–1099.
36. Mestecky, J., Moro, I., Kerr, M.A., and Woof, J.M. 2005. Mucosal immunoglobulins. In *Mucosal immunology.* 3rd edition. J. Mestecky, et al., editors. Elsevier Academic Press. Amsterdam, The Netherlands. 153–181.
37. Kilian, M., and Russell, M.W. 2005. Microbial evasion of IgA functions. In *Mucosal immunology.* 3rd edition. J. Mestecky, et al., editors. Elsevier Academic Press. Amsterdam, The Netherlands. 291–303.
38. van Dixhoorn, M.G., et al. 2000. Combined glomerular deposition of polymeric rat IgA and IgG aggravates renal inflammation. *Kidney Int.* **58**:90–99.
39. Nieuwhof, C., Kruytzer, M., Frederiks, P., and van Breda Vriesman, P.J.C. 1998. Chronicity index and mesangial IgG deposition are risk factors for hypertension and renal failure in early IgA nephropathy. *Am. J. Kidney Dis.* **31**:962–970.
40. Sedivá, A., et al. 1999. Binding sites for carrier-immobilized carbohydrates in the kidney: implication for the pathogenesis of Henoch-Schönlein purpura and/or IgA nephropathy. *Nephrol. Dial. Transplant.* **14**:2885–2891.
41. Emancipator, S.N., and Lamm, M.E. 1989. Biology of disease. IgA nephropathy: Pathogenesis of the most common form of glomerulonephritis. *Lab. Invest.* **60**:168–183.
42. Emancipator, S.N. 1998. IgA nephropathy and Henoch-Schönlein syndrome. In *Heptinstall's pathology of the kidney.* J.C. Jennette, J.L. Olson, M.M. Schwartz, and F.G. Silva, editors. Lippincott Williams & Wilkins. Philadelphia, Pennsylvania, USA. 479–539.
43. Jennette, J.C. 1988. The immunohistology of IgA nephropathy. *Am. J. Kidney Dis.* **12**:348–352.
44. Lomax-Smith, J.D., Woodroffe, A.J., Clarkson, A.R., and Seymour, A.E. 1985. IgA nephropathy — accumulated experience and current concepts. *Pathology.* **17**:219–224.
45. Vanderlugt, C.L., et al. 1998. The functional significance of epitope spreading and its regulation by co-stimulatory molecules. *Immunol. Rev.* **164**:63–72.
46. Bassing, C.H., Swat, W., and Alt, F.W. 2002. The mechanism and regulation of chromosomal V(D)J recombination. *Cell.* **109**(Suppl.):S45–S55.
47. Tonegawa, S. 1983. Somatic generation of antibody diversity. *Nature.* **302**:575–581.
48. Xu, J.L., and Davis, M.M. 2000. Diversity in the CDR3 region of V(H) is sufficient for most antibody specificities. *Immunity.* **13**:37–45.
49. Rajewsky, K. 1996. Clonal selection and learning in the antibody system. *Nature.* **381**:751–758.
50. McKean, D., et al. 1984. Generation of antibody diversity in the immune response of BALB/c mice to influenza virus hemagglutinin. *Proc. Natl. Acad. Sci. U. S. A.* **81**:3180–3184.
51. Kubagawa, H., Burrows, P.D., Grossi, C.E., Mestecky, J., and Cooper, M.D. 1988. Precursor B cells transformed by Epstein-Barr virus undergo sterile plasma-cell differentiation: J-chain expression without immunoglobulin. *Proc. Natl. Acad. Sci. U. S. A.* **85**:875–879.
52. Matousovic, K., et al. 2006. IgA1-containing immune complexes in the urine of IgA nephropathy patients. *Nephrol. Dial. Transplant.* **21**:2478–2484.